Supplement of E&G Quaternary Sci. J., 69, 201–223, 2020
https://doi.org/10.5194/egqsj-69-201-2020-supplement

Open Access E&G Quaternary Science Journal

Supplement of

Proposing a new conceptual model for the reconstruction of ice dynamics in the SW sector of the Scandinavian Ice Sheet (SIS) based on the reinterpretation of published data and new evidence from optically stimulated luminescence (OSL) dating

Christopher Lüthgens et al.

Correspondence to: Margot Böse (m.boese@fu-berlin.de)

Introduction

This supplementary document provides complementary details to the basic information provided in the main text about the luminescence dating approach applied, and about the sedimentological and stratigraphic context for the two new sites investigated in this study. All laboratory analyses described here were conducted at the Vienna Laboratory for Luminescence dating (VLL). This included mechanical and chemical sample preparation steps, high-resolution gamma spectrometry measurements, all luminescence analyses, and final age calculation. For all stratigraphic and geomorphological implications please see the text in the main paper.

Sample preparation

The luminescence samples were delivered to the VLL in closed, light-tight plastic cylinders. All subsequent sample preparation steps were conducted under subdued red-light conditions according to the procedures described by e.g. Hardt et al. (2016) and Lüthgens et al. (2017). Samples were opened and the outer few centimetres of material exposed to daylight during sampling were carefully removed. Only the inner parts of the cores were used for all subsequent preparation steps. Separates of pure quartz (in the grain size fraction of 170 – 250 µm for Jänschwalde and 220 – 250 µm for Müncheberg) were extracted by a procedure including drying of the sediment at 50°C, dry sieving, leaching of carbonates (10% HCl) and organics (10% H_2O_2), dispersion of aggregates and clay coatings ($Na_2C_2O_4$, 0.01 N), and density separation (LST Fastfloat at 2,68 g/cm^3).

Samples for radionuclide analyses were taken from the direct surroundings of the luminescence samples and were first dried, manually homogenized (gentle crushing of aggregates) and subsequently sealed in Marinelli beakers (500ml equivalent to ~1kg dry weight of sample material) and stored for at least a month before measurement to establish secondary secular Radon (Rn) equilibrium.

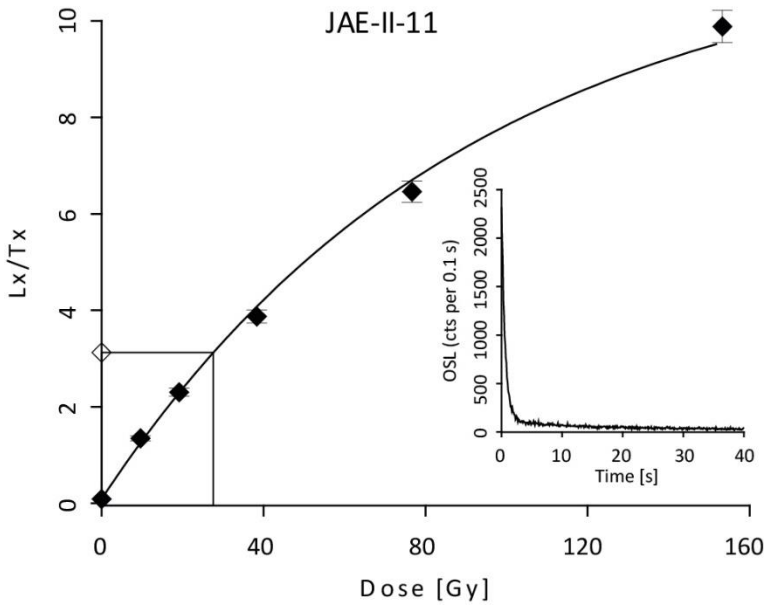

Figure S1: Representative dose response curve (sensitivity corrected luminescence signal (Lx/Tx) plotted vs. dose (Gy)) and decay curve for an aliquot of sample JAE-II-11. Plots generated using the R-luminescence package of Kreutzer et al. (2012).

Experimental setup

Determination of the equivalent dose

Quartz was used as a dosimeter for all measurements, because the luminescence signal of quartz is known to be reset by daylight exposure much faster than that of feldspar. In glaciofluvial sediments, incomplete bleaching (incomplete resetting of the luminescence signal prior to burial) is known to occur frequently (e.g. Lüthgens et al. 2010a/b, 2011, Hardt et al. 2016) and leads to age overestimation if not detected and corrected for. We measured quartz grains in the grain size fraction of 170 – 250 µm (Jänschwalde) and 220 – 250 µm (Müncheberg). The aliquot size was 1 mm for the Jänschwalde samples, and 2 mm for the Müncheberg samples, which results in an average of 15 - 25 grains per disc. In previous tests on Weichselian glaciofluvial material on single grains we observed that only 3 – 5 % of the quartz grains emit a significant luminescence signal (Lüthgens et al., 2010b; Hardt et al., 2016). Thus, the measurements were done on a quasi-single grain level, which is an important prerequisite when working on poorly bleached (glaciofluvial) material. All measurements were carried out at the VLL on Risø DA-20 automated luminescence reader systems (Bøtter-Jensen et al. 2000, 2003). The quartz emission from multigrain aliquots was stimulated using blue (470 nm) light emitting diodes (LEDs) and detected through a 7.5-mm Hoya U340 filter by a photomultiplier. For necessary irradiation steps all reader systems are equipped with a $^{90}Sr/^{90}Y$ beta source delivering a dose rate of approximately 0.1 Gy/s. The suitability of the applied single aliquot regenerative dose (SAR) protocol (Murray & Wintle 2000 & 2003, Wintle & Murray 2006) using a preheat of 10 s @ 240 °C and a cutheat for another 10 s @ 220 °C was confirmed by dose recovery experiments on selected samples which yielded recovery ratios (measured/given dose) within 10 % of unity.

Some authors recommend early background subtraction (EBG) to ensure the isolation of the fast component of the quartz OSL signal (Ballarini et al., 2007, Cunningham and Wallinga, 2010). Quartz from the study area is known to be fast component dominated (Lüthgens et al. 2010a, 2010b, 2011, Hardt et al. 2016), but we still compared dose distributions using EBG vs. late background subtraction (LBG) for both, dose recovery experiments and natural equivalent dose

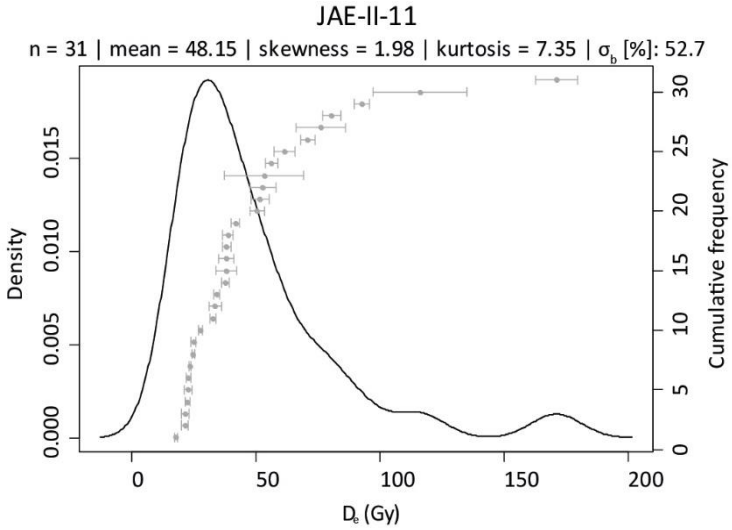

Figure S2: Representative equivalent dose distribution and basic statistical parameters for sample JAE-II-11. Please note that the distribution is right-skewed and shows an overdispersion of >50%, which indicates that the sample was not fully bleached before deposition. Plot generated using the R-luminescence package of Kreutzer et al. (2012).

measurements. In all cases, LBG yielded results in agreement with the EBG-approach, but with a significantly higher yield of equivalent dose values than obtained for the EBG-approach. Therefore, the first 0.9 s of stimulation were used for signal integration, whereas the last 10 s served as background. Aliquots were accepted when fulfilling the following rejection criteria: recycling ratio <15% and maximum recuperated dose < 5% of the natural signal (both including uncertainty). A representative dose response curve and a decay curve are provided in figure S1.

Determination of the dose rate

Activities of naturally occurring radionuclides (^{238}U and ^{232}Th decay chains, as well as ^{40}K) within the sediment were determined by high-resolution, low-level gamma spectrometry. To achieve a preferable signal to noise ratio, each sample was measured for 24 hours at the VLL using a Canberra HPGe (40 % n-type) detector. The external dose rate was calculate based on the results from radionuclide analysis (table S1), using the conversion factors of Adamiec & Aitken (1998) and the β-attenuation factors of Mejdahl (1979). An average water content 8 ±4 % was estimated for the time of burial, because of the good drainage within the sandy deposits and no water-impermeable layers close below the sampling spots. The uncertainty assigned to the water content was propagated to the final dose rate and age calculation.

Site	Sample	Depth (m)	U^{238} (Bq/kg)[1]	Th^{232} (Bq/kg)[1]	K^{40} (Bq/kg)[1]	Grain size (µm)	Dose rate (Gy/ka)[2]	(n)	MAM paleodose (Gy)[3]	Age (ka)[4]	Average age (ka)[5]
Jänschwalde	JAE-II-10	4.7	13.48 ±0.37	13.07 ±0.42	373.61 ±8.12	170-250	1.38 ±0.09	25	45.8 ±5.5	**33 ±4**	**30 ±4**
	JAE-II-11	3.7	4.88 ±0.16	4.55 ±0.18	194.32 ±4.31	170-250	0.90 ±0.07	31	23.9 ±3.2	**27 ±4**	
	JAE-II-12	2.1	5.05 ±0.18	4.31 ±0.18	203.33 ±4.51	170-250	0.95 ±0.07	11	51.6 ±11.4	<54 ±13*	
	JAE-II-13	1.6	5.93 ±0.19	5.08 ±0.20	173.24 ±3.86	170-250	0.91 ±0.07	50	28.8 ±3.1	**32 ±4**	
Müncheberg	WIL-I-1	8.4	7.36 ±0.22	6.43 ±0.35	229.69 ±1.28	220-250	0.95 ±0.08	32	28.0 ±2.9	**30 ±3**	**31 ±4**
	WIL-I-2	7.4	7.10 ±0.20	6.00 ±0.33	253.00 ±1.22	220-250	0.99 ±0.08	18	29.8 ±4.6	**30 ±5**	
	WIL-II-2b	5.3	6.40 ±0.21	5.29 ±0.30	185.42 ±1.12	220-250	0.92 ±0.07	20	26.8 ±4.0	**29 ±5**	
	WIL-II-3	3.7	7.13 ±0.26	6.56 ±0.41	205.39 ±1.81	220-250	0.92 ±0.07	17	33.2 ±6.1	**35 ±5**	
	WIL-III-1	0.7	4.87 ±0.2	4.29 ±0.29	147.88 ±1.53	220-250	0.76 ±0.06	7	71.8 ±17.9	<95 ±24*	

Table S1: Summary of results from OSL dating

[1]Activities determined by low-level gamma spectrometry (Canberra n-type detector, ~40 % efficiency) at the VLL.

[2] Overall environmental dose rates based on the provided radionuclide activities and calculated using 8±4% water content and using conversion factors of Adamiec & Aitken (1998) and β-attenuation factors of Mejdahl (1979); cosmic dose rate determined according to Prescott & Stephan (1982) and Prescott & Hutton (1994).

[3] D_e calculated using the three parameter minimum age model (MAM) according to Galbraith et al., (1999) using the R Luminescence package (Kreutzer et al., 2012) and a threshold of 0.2 for the sigma_b parameter.

[4] Calculated using the software ADELE (Kulig, 2005). Ages in bold used for the calculation of the average ages.

The cosmic dose rate was determined according to Prescott & Stephan (1982) and Prescott & Hutton (1994), taking into account the geographical position of the sampling spot (longitude, latitude, and altitude), the depth below surface, as well as the average density of the sediment overburden. An uncertainty of 10% was assigned to the calculated cosmic dose rate. The resulting overall dose rate is provided in table S1.

Results

The majority of samples showed good performance with regard to the quality criteria of the SAR protocol and yielded sufficient numbers of equivalent dose values for further data evaluation. A representative dose distribution is shown in figure S2. All these samples show clearly right-skewed dose distributions and overdispersion values typically ranging from >30 % to >50 %. Both factors in combination are strong indicators for significant incomplete bleaching present in the samples. Consequently, the three parameter minimum age model of Galbraith et al. (1999) was applied to calculate paleodose values for the samples. The threshold for the minimum expected overdispersion was set to 20 % as based on the overdispersion parameters observed from few well bleached samples from the broader research area in earlier studies (Lüthgens et al. 2011, Hardt et al. 2016). For two samples (JAE-II-13 & WIL-III-1) the yield of obtained equivalent dose values was very low. This was caused by a high number of aliquots showing natural doses above the highest laboratory dose administered in the SAR protocol, which can be interpreted to have been caused by extremely poor incomplete bleaching. While sample JAE-II-13 showed at least few individual equivalent dose values in line with the equivalent doses from the over- and underlying samples, sample WIL-III-1 did not show any dose values even close to those expected.

Tests using significantly higher maximum laboratory doses confirmed that trend and even showed large numbers of aliquots with oversaturation effects (natural dose not

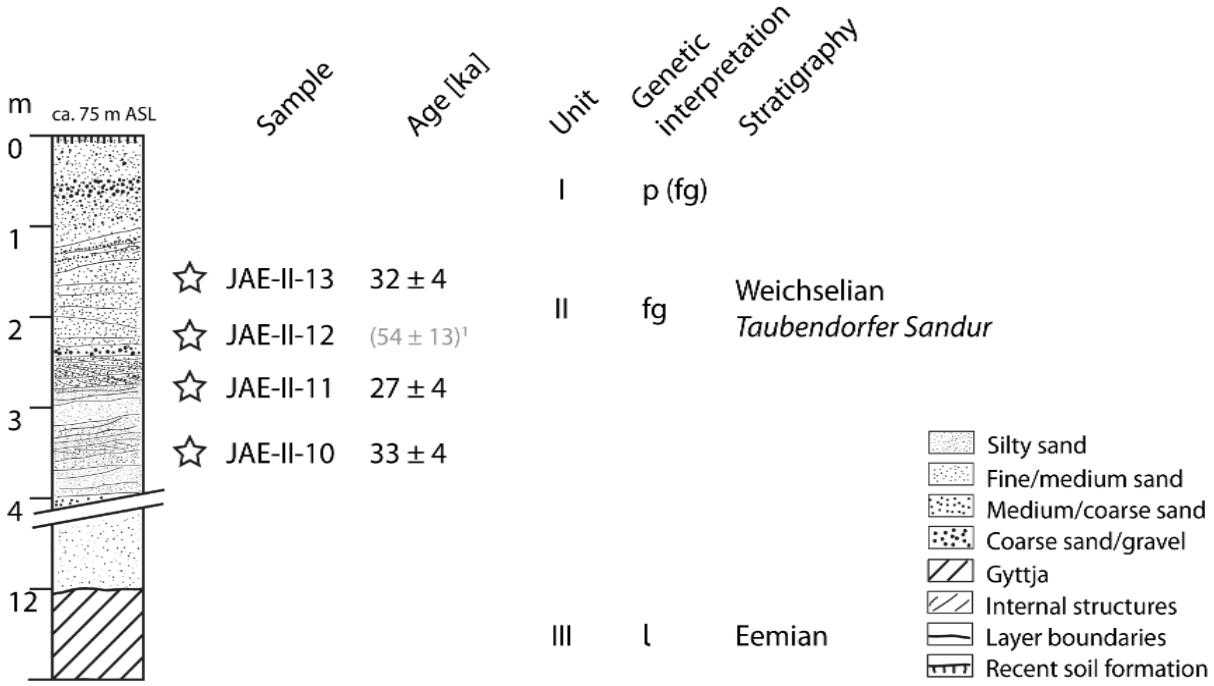

Figure S3: Stratigraphic log for the sampling site Jänschwalde and OSL ages in stratigraphic context. Genetic interpretation codes: p – periglacial; fg - glaciofluvial; l – limnetic. [1] Age excluded from mean age calculation.

intersecting with the saturated laboratory dose response curve). Only maximum ages could be calculated for samples JAE-II-13 & WIL-III-1, and they were excluded from all further evaluation. All age and dose rate calculation was done using the software ADELE (Kulig 2005).

Reliability of the data

The ages determined for all samples of each site are in good agreement within error, which reliably demonstrates that effects of incomplete signal resetting were successfully identified and corrected for by the applied SAR protocol and the subsequent statistical data evaluation approach. Average ages were calculated for each site (See supplementary table 1), which are in excellent agreement within error and line up perfectly with results from sites ascribed to the same ice advance in the research area as described in detail in the main manuscript.

Ages in stratigraphic context

All stratigraphic and geomorphological implications of the new ages are described in the text of the main paper. Sedimentological details are summarized in figures S3 and S4.

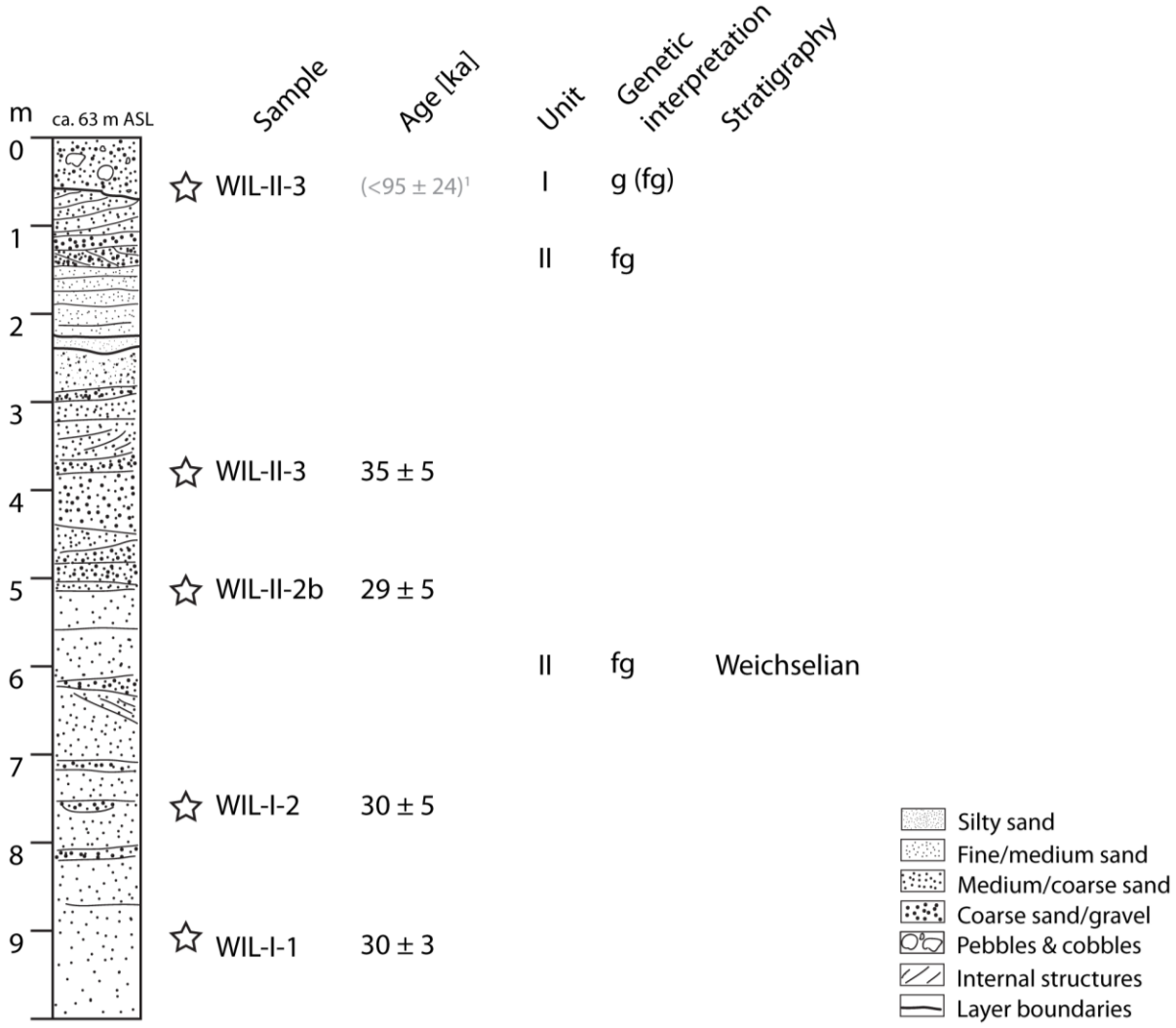

Figure S4: Stratigraphic log for the sampling site Müncheberg “Wildermann” and OSL ages in stratigraphic context. Genetic interpretation codes: g – glacigenic; fg - glaciofluvial. [1] Age excluded from mean age calculation.

References

Adamiec, G., Aitken, M., 1998. Dose-rate conversion factors: update. Ancient TL 16, 37-50.

Ballarini, M., Wallinga, J., Wintle, A.G., Bos, A.J.J., 2007. A modified SAR protocol for optical dating of individual grains from young quartz samples. Radiation Measurements 42, 360-369.

Bøtter-Jensen, L., Andersen, C., Duller, G., Murray, A., 2003. Developments in radiation, stimulation and observation facilities in luminescence measurements. Radiation Measurements 37, 535-541.

Bøtter-Jensen, L., Bulur, E., Duller, G., Murray, A., 2000. Advances in luminescence instrument systems. Radiation Measurements 32, 523-528.

Cunningham, A., Wallinga, J., 2010. Selection of integration time intervals for quartz OSL decay curves. Quaternary Geochronology 5, 657-666.

Galbraith, R., Roberts, R., Laslett, G., Yoshida, H., Olley, J., 1999. Optical dating of single and multiple grains of Quartz from Jinmium rock shelter, northern Australia: Part I, experimental design and statistical models. Archaeometry 41, 339-364.

Hardt, J., Lüthgens, C., Hebenstreit, R., Böse, M., 2016. Geochronological (OSL) and geomorphological investigations at the presumed Frankfurt ice marginal position in northeast Germany. Quaternary Science Reviews 154, 85-99.

Krbetschek, M., Götze, J., Dietrich, A., Trautmann, T., 1997. Spectral information from minerals relevant for luminescence dating. Radiation Measurements 27, 695-748.

Kreutzer, S., Schmidt, C., Fuchs, M., Dietze, M., Fuchs, M., 2012. Introducing an R package for luminescence dating analysis. Ancient TL 30, 1-8.

Kulig G., 2005. Erstellung einer Auswertesoftware zur Altersbestimmung mittels Lumineszenzverfahren unter spezieller Berücksichtigung des Einflusses radioaktiver Ungleichgewichte in der ^{238}U-Zerfallsreihe. 35 p., B.Sc. thesis, Freiberg (Technische Universität Bergakademie Freiberg).

Lüthgens, C., Neuhuber, S., Grupe, S., Payer, T., Peresson, M., Fiebig, M., 2017. Geochronological investigations using a combination of luminescence and cosmogenic nuclide burial dating of drill cores from the Vienna Basin. Zeitschrift der Deutschen Gesellschaft für Geowissenschaften 168, 115-140.

Lüthgens, C., Böse, M., Krbetschek, M., 2010a. On the age of the young morainic morphology in the area ascribed to the maximum extent of the Weichselian glaciation in north-eastern Germany. Quaternary International 222, 72-79.

Lüthgens, C., Böse, M., Preusser, F., 2011. Age of the Pomeranian ice-marginal position in northeastern Germany determined by Optically Stimulated Luminescence (OSL) dating of glaciofluvial sediments. Boreas 40, 598-615.

Lüthgens, C., Krbetschek, M., Böse, M., Fuchs, M.C., 2010b. Optically stimulated luminescence dating of fluvioglacial (sandur) sediments from north-eastern Germany. Quaternary Geochronology 5, 237-243.

Mejdahl, V., 1979. Thermoluminescence dating: beta attenuation in quartz grains. Achaeometry 21, 61-73.

Murray, A. & Wintle, A., 2000. Luminescence dating of quartz using an improved single-aliquot regenerative-dose protocol. Radiation Measurements, 32: 57-73.

Murray, A. & Wintle, A., 2003. The single aliquot regenerative dose protocol: potential for improvements in reliability. Radiation Measurements, 37: 377-381.

Prescott, J., Hutton J., 1994. Cosmic ray distributions to dose rates for luminescence and ESR dating: large depths and long-term variations. Radiation Measurements 23, 497-500.

Prescott, J., Stephan, L., 1982. The contribution of cosmic radiation to the environmental dose for thermoluminescent dating - Latitude, altitude and depth dependencies. PACT 6, 17-25.

Wintle, A. & Murray, A., 2006. A review of quartz optically stimulated luminescence characteristics and their relevance in single-aliquot regeneration dating protocols. Radiation Measurements, 41: 369-391.